

H₃dotasa (= (α RS)- α -(Carboxymethyl)-1,4,7,10-tetraazacyclododecane-1,4,7,10-tetraacetic Acid), an Asymmetrical Derivative of H₄dota (= 1,4,7,10-Tetraazacyclododecane-1,4,7,10-tetraacetic Acid) Substituted at One Acetate Pendant Arm: ¹H-NMR and Potentiometric Studies of the Ligand and Its Lanthanide(III) Complexes

by João P. André*^a), Ernö Brücher^b), Robert Kiraly^b), Rui A. Carvalho^c), Helmut Mäcke^d), and Carlos F. G. C. Geraldes*^c)

^a) Centro de Química, Campus de Gualtar, Universidade do Minho, P-4710-057 Braga
(e-mail: jandre@quimica.uminho.pt)

^b) Department of Inorganic and Analytical Chemistry, University of Debrecen, H-4010 Debrecen

^c) Department of Biochemistry, Faculty of Science and Technology, NMR Center and Center of Neurosciences and Cell Biology, University of Coimbra, P.O. Box 3126, P-3001-401 Coimbra
(phone: + 35 123 985 36 08; e-mail: geraldes@ci.uc.pt)

^d) Division of Radiological Chemistry, Institute of Nuclear Medicine, University Hospital, Petersgraben 4, CH-4031 Basel

Dedicated to Professor André E. Merbach on the occasion of his 65th birthday

The ligand H₃dotasa (= (α RS)- α -(carboxymethyl)-1,4,7,10-tetraazacyclododecane-1,4,7,10-tetraacetic acid) is a H₄dota-like macrocyclic ligand with a carboxymethyl CH₂COOH substituent at the C(α) atom of one of the four acetate pendant arms of H₄dota (= 1,4,7,10-tetraazacyclododecane-1,4,7,10-tetraacetic acid), present as a racemic mixture of (α R) and (α S) enantiomers. The protonation constants of the ligand were determined by potentiometry, giving values close to those of H₄dota except for the extra pK₇ value of 5.35 assigned to protonation of the extra carboxylate group in the α -substituted (=succinic acid) pendant arm. The ¹H-NMR spectra of H₃dotasa at different pH values are too complex to allow the determination of its microscopic protonation scheme, due to the presence of multiple isomeric structures in solution. The thermodynamic stability constant of its Gd³⁺ chelate was determined by a potentiometric method, and the value obtained, log K_{ML} = 27.2 (0.2), is higher than for the [Gd(dota)(OH₂)]⁻ complex. The solution structure of the asymmetric Ln³⁺ chelates of dotasa was studied by ¹H-NMR spectroscopy, indicating the presence of four isomers, corresponding to the combination of the antiprismatic (*M*) and twisted antiprismatic (*m*) helicities of the pendant arms and to the (α R) and (α S) configurations at the substituted pendant arm. The *m*/*M* isomer ratio decreases along the lanthanide series, with the *m* isomer decreasing from 90% at La to ca. 50% from Eu–Lu. This shows that the expected *m* isomer population of the [Gd(dotasa)(OH₂)]²⁻ complex is higher than for the unsubstituted [Gd(dota)(OH₂)]⁻ (ca. 15%) but lower than for a Gd³⁺ chelate of an $\alpha,\alpha',\alpha'',\alpha'''$ -tetrasubstituted (*RRRR*)-configured dota (ca. 70%). Thus the stabilization of the *m* isomer by C. monosubstitution at the dota acetate pendant arm in [Gd(dotasa)(OH₂)]²⁻ is responsible for its increased H₂O-exchange rate and higher relaxivity.

1. Introduction. – Due to their paramagnetic, luminescent, and radioactive properties, the trivalent lanthanide ions, Ln³⁺, have found a variety of applications in biomedical sciences [1–5]. The high toxicity of the free ion form can be circumvented by *in vivo* application in the form of stable chelates.

Most magnetic-resonance-imaging (MRI) contrast agents are gadolinium(III) chelates of polyaminopolycarboxylate-like ligands. In particular, the tetraazacyclodo-

decane polycarboxylic acid ligands proved to be suitable chelating agents in regard of the thermodynamic and kinetic stability of their Gd^{3+} chelates [6][7]. H_4dota (=1,4,7,10-tetraazacyclododecane-1,4,7,10-tetraacetic acid) became a popular ligand in the last two decades due to its strong capability to encapsulate the Gd^{3+} ion, while allowing the cation to keep one H_2O molecule in the inner coordination sphere [8]. This H_2O molecule conveys the paramagnetic effects of the metal ion to the bulk water. Many attempts have been made to improve the paramagnetic T_1 relaxation effect of the Gd^{3+} ion on the protons of bulk water, by optimizing the molecular parameters which determine the relaxivity of those protons, while preserving a dota-like coordination pattern within the chelate [7]. In a previous work [9] we reported the synthesis and physicochemical characterization of the ligand H_5dotasa (= (αRS)- α -(carboxymethyl)-1,4,7,10-tetraazacyclododecane-1,4,7,10-tetraacetic acid = '1,4,7,10-tetraazacyclododecane-1-[(R,S)-succinic acid]-4,7,10-triacetic acid'; Fig. 1), which has a succinic acid derived pendant arm, resulting from the attachment of a carboxymethyl (CH_2COOH) substituent at the C(α) atom of one of the four acetate pendant arms of H_4dota , giving a racemic mixture of (αR) and (αS) enantiomers. This extra carboxylate of H_5dotasa relative to H_4dota , which remains free upon coordination to the Gd^{3+} ion in the $[\text{Gd}(\text{dotasa})(\text{OH}_2)]^{2-}$ chelate, was shown to be responsible for an increase in the H_2O -exchange rate and in the size of the species tumbling in solution with a concomitant overall improvement of *ca.* 30% in its relaxivity in relation to $[\text{Gd}(\text{dota})(\text{OH}_2)]^-$. Additionally, the extra carboxylate group proved to be convenient for coupling the chelate to other molecules [10], which is of extreme importance regarding the targeting of organs.

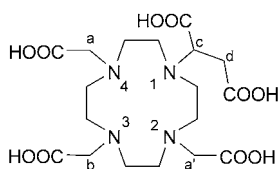


Fig. 1. Structure of ligand H_5dotasa . Arbitrary numbering and labelling.

The Ln^{3+} complexes of H_4dota -like chelating agents exhibit a variety of conformational and coordination isomers which may display dynamic behavior on the NMR time scale [6][7][11]. The isomers of their Gd^{3+} chelates have been found to have different relaxivity properties [12]. Thus, in the present work, we studied the acid-base properties of H_5dotasa , as well as the thermodynamic stability and structure of some of its Ln^{III} chelates in aqueous solution, both by ^1H -NMR and potentiometry.

2. Results and Discussion. – 2.1. *Ligand Protonation Studies: Potentiometry and NMR.* Table 1 summarizes the protonation constants of H_5dotasa , obtained in this study from potentiometric titrations at 25° in the presence of different support electrolytes. These were compared with the corresponding literature values for H_4dota [13–15]. The protonation constants of H_5dotasa were not much different from those of H_4dota , indicating that the presence of an extra carboxylic acid group that is not directly attached to an N-atom of the ring has very little effect on the protonation constants of the remaining ionizable moieties of the ligand.

Table 1. Protonation Constants ($\log K_i$) of $H_5\text{dotasa}$ and $H_4\text{dota}$ at 25° Obtained by Potentiometry

$\log K_i$	$H_5\text{dotasa}$		$H_4\text{dota}$		
	0.1M Me_4NCl	0.5M Me_4NNO_3	0.1M Me_4NCl [15]	0.1M Me_4NCl [14]	0.1M Me_4NNO_3 [13]
$\log K_1$	10.99 (0.02)	11.17	11.74	11.73	12.09
$\log K_2$	9.18 (0.02)	9.38	9.76	9.40	9.68
$\log K_3$	5.35 (0.02)	5.25	4.68	4.50	4.55
$\log K_4$	4.40 (0.02)	4.21	4.11	4.19	4.13
$\log K_5$	3.75 (0.02)	3.28	2.37	–	–
$\log K_6$	2.93 (0.02)	–	–	–	–
$\log K_7$	1.8 (0.04)	–	–	–	–
$\log K_8$	1.2 (0.06)	–	–	–	–

Although potentiometry cannot provide information on the microscopic sequence of protonation of the basic sites of the ligand, a simple comparison with $H_4\text{dota}$ leads to the assumption that the third protonation in $H_5\text{dotasa}$ occurs mainly in the extra carboxylate, and only at the fourth protonation, the ligand attains again a $H_4\text{dota}$ -like protonation pattern [16]. This hypothesis could be in principle analyzed by studying the microscopic protonation sequence of $H_5\text{dotasa}$, based on a $^1\text{H-NMR}$ pH titration of the ligand by using K^+ as the counter-ion, if this cation does not bind significantly to macrocyclic ligands of this type [16]. It is well-known that changes in $^1\text{H-NMR}$ chemical shifts can indicate successive protonation sites of the various basic groups of the ligand because the protonation of donor atoms generally results in a deshielding of the non-labile H-atoms nearby. Under conditions of fast proton exchange among the various protonated species, H_nL , the observed averaged chemical shift of nucleus i is given by $\delta_{\text{obs}}^i = \sum_n \delta_n^i X_{H_nL}$, where δ_n^i are the intrinsic chemical shifts of the H_nL species and X_{H_nL} is the mole fraction of each species. With the protonation constants obtained by potentiometry, the δ_n^i values can be calculated *via* a multiple linear regression program, which minimizes the sums of the squares of the deviation between the observed and calculated δ_{obs}^i values [17]. Then, these intrinsic shifts can be used to calculate the percentage protonations at the N- (f_N) and O-sites (f_O) at each pH, by a well-known empirical procedure based on the additivity of the protonation shifts at the various basic sites. According to this procedure, the observed shifts of the nonexchangeable ligand protons δ_{obs}^i are a function of intrinsic shifts of the fully deprotonated form of the ligand, δ_0^i , the fractions of protonation f_N and f_O , and the shielding constants C_O (shift due to the carboxylate protonation), C_N and $C_{N'}$ (shift due to protonation of an N-atom in the α - and β -position, respectively), all relative to the CH_2 group under study. This procedure has been applied with success to many linear and macrocyclic polyamino carboxylate and -phosphonate ligands [16–22], including $H_4\text{dota}$ [16][20]. All the values of f_N and f_O calculated for this ligand clearly show that two N-atoms of $H_4\text{dota}$ are protonated first (at $n=2$, $f_N \approx 0.50$, $f_O = 0$), and only then the four carboxylate groups are increasingly protonated in the same amounts (at $n=6$, $f_N \approx 0.50$, $f_O = 1.00$), as expected for the ligand symmetry [16][20].

This symmetry is broken for $H_5\text{dotasa}$ due to the presence of the extra carboxymethyl group in one of the pendant arms. Thus, the $^1\text{H-NMR}$ spectra of $H_5\text{dotasa}$ are very complex at all pH values studied (pH 12.0–0.6) at 25° and 70°. Even the COSY plots obtained at various pH values and both temperatures did not allow full

assignment of the resonances, which made it impossible to obtain $^1\text{H-NMR}$ pH titration curves for H_5dotasa , and thus prevented a full study of its protonation scheme. The COSY experiments were performed at 25° and 70° , at pH values corresponding to the predominance of increasingly protonated states of the ligand, namely at pH 12.0 (L), 10.64 (HL), 8.95 (H_2L), 4.27 (H_3L), 3.50 (H_4L), 2.10 (H_5L) and 0.60 (H_6L). They allowed unequivocal assignment of the resonances from the (carboxymethyl)-substituent CHCH_2 protons of H_5dotasa which should give a well-resolved *ABX* pattern. In fact, a large number of *ABX* patterns were obtained from this moiety: between 6 and 8 for the forms L up to H_4L , and 3 for H_5L and H_6L at 25° . At 70° , this number decreased to 3 for L, HL, H_3L , and H_5L , to 4 for H_4L , and did not decrease for H_2L . The complexity of the spectra prevented any further assignments, except for the location of some *AB* patterns of the methylene protons of the unsubstituted acetate arms.

The shift of a given resonance of the (carboxymethyl)-substituent CHCH_2 protons of H_5dotasa was found to be pH independent at pH 12–8.95, and only started to increase for lower pH values, indicating that the first two protonations are distributed among the three N-atoms N(2), N(3), and N(4) bound to the acetate arms, thus excluding N(1) (see *Fig. 1*), and only at lower pH values, the carboxylate groups, including the $\text{C}(\alpha)$ substituent, are protonated.

The complexity of the $^1\text{H-NMR}$ spectra of the unprotonated and protonated forms of H_5dotasa , reflected not only in the large number of resonances of non-equivalent protons of the unsymmetrical ligand, but especially in the presence of 3 to 8 resonances for each type of proton, is an indication of the presence of a large number of ligand topomers in solution, with exchange processes between them accounting for the partial simplification of the spectra at high temperature. These topomers should have high internal rigidity due to the presence of internal H-bonds between protonated N-atoms and carboxylates, and should differ in the relative orientation of the carboxylate arms relative to the tetraaza ring and the (αR)/(αS) configuration at the substituted $\text{C}(\alpha)$ in the pendant arm. However, a detailed study of their structure and dynamics was not undertaken. In the solid state, diprotonated H_4dota adopts a [3.3.3.3] square conformation of fourfold symmetry with all the carboxylate arms located on the same side of the tetraaza ring [8]. However, even for this symmetrical ligand, the $^1\text{H-NMR}$ spectrum of the H_6L form in strong acidic media becomes quite broad at low temperature (278 K), reflecting the slowing down of its intramolecular dynamic processes [16]. The relatively complex but well-defined $^1\text{H-NMR}$ spectra obtained for the tetramethyl-substituted ligand $\text{H}_4\text{m}_4\text{dota}$ (with four Me groups at the tetraaza macrocyclic ring), the tetramethyl-substituted ligand H_4dotma (four Me substituents at $\text{C}(\alpha)$ of the acetate arms), and the octamethyl-substituted ligand $\text{H}_4\text{m}_4\text{dotma}$ (both types of substitutions) in acidic media have been interpreted by the presence of two slowly exchanging elongated (less symmetric than [3.3.3.3]) conformations for the H_4L and H_6L forms of these ligands [23].

2.2. Complexation Studies by Potentiometry. Some spectrophotometric experiments were carried out in the system $\text{Ce}^{3+}/\text{H}_5\text{dotasa}$ and found that the absorption bands of the Ce^{3+} ion and of the $[\text{Ce}(\text{dotasa})(\text{OH}_2)]^{2-}$ complex are overlapping. Thus, they are not suitable for complex stability calculations, but this system is a useful detector of the complex formation. The formation rate of $[\text{Ce}(\text{dotasa})(\text{OH}_2)]^{2-}$ is expectably lower

than that of $[\text{Gd}(\text{dotasa})(\text{OH}_2)]^{2-}$ [24]. This means that, at the time after which the UV/VIS spectrum of the system $\text{Ce}^{3+}/\text{H}_5\text{dotasa}$ is unchanged, the system $\text{Gd}^{3+}/\text{H}_5\text{dotasa}$ is also in equilibrium. This helped us to design a potentiometric determination of the stability constant for the complex $[\text{Gd}(\text{dotasa})(\text{OH}_2)]^{2-}$ by using an ‘out of cell’ method. The value obtained, $\log K_{\text{ML}} = 27.2$ (0.2), is higher than the one of $[\text{Gd}(\text{dota})(\text{OH}_2)]^-$ ($\log K_{\text{ML}} = 25.3$ [14]). This finding is probably due to the extra negative charge of the completely deprotonated ligand.

2.3. *NMR Studies of the $[\text{Ln}(\text{dotasa})]^{2-}$ Complexes.* $^1\text{H-NMR}$ is quite useful in the solution study of the isomers of the Ln^{3+} complexes of H_4dota and its derivatives [6] [7]. The high symmetry of H_4dota leads to the well-known presence of only two isomers of the $[\text{Ln}(\text{dota})(\text{OH}_2)]^-$ chelates in solution, with square antiprismatic (M) and twisted antiprismatic (m) geometries [8] [25–28]. These two isomers have the same [3.3.3.3] square conformation with fourfold symmetry of the tetraazacyclododecane ring, where all its ethylenic groups adopt a δ or λ conformation, thus leading to conformations of clockwise or counterclockwise helicity, $\lambda\lambda\lambda\lambda$ or $\delta\delta\delta\delta$. They only differ in the layout of the four acetate pendant arms, resulting from rotations around the $\text{N-CH}_2\text{-COO}$ bonds, with either a clockwise (Λ) or counterclockwise (Δ) helicity. These lead to the two diastereoisomers referred to above, with separate NMR resonances, each of which is an enantiomer pair: the square antiprismatic (M) geometry results from the opposite helicity of the tetraaza ring and the acetate arms ($\Delta(\lambda\lambda\lambda\lambda)$ or $\Lambda(\delta\delta\delta\delta)$), while the twisted antiprismatic (m) geometry has the same ring and acetate helicity ($\Lambda(\lambda\lambda\lambda\lambda)$ or $\Delta(\delta\delta\delta\delta)$). Thus, M and m differ in the value and sign of the twist angle α between the diagonals of the parallel squares formed by the four N-atoms and the four carboxylate O-atoms in the coordination polyhedron of the dota chelates, with typical values of $\alpha \approx +35^\circ$ and $\alpha \approx -15^\circ$, respectively, found from crystallographic structures [7]. The isomer M shows a wider paramagnetic shift range than m throughout the lanthanide series. The isomer m is dominant relative to M for the early Ln^{3+} chelates ($\text{Ln} = \text{La} - \text{Pr}$), but M becomes dominant for the smaller ions ($\text{Ln} = \text{Eu} - \text{Lu}$) [28].

The H_5dotasa ligand used in this study is an asymmetrical derivative of H_4dota , with one of the four acetate $\text{C}(\alpha)$ atoms substituted with a carboxymethyl group. This introduces a chiral center in the ligand and a site of asymmetry in the complexes which doubles the number of possible isomeric species in solution. As in our study the ligand H_5dotasa was obtained as a racemic mixture of the (αR) and (αS) enantiomers [9], the complete identification of all the possible stereoisomers requires indication of the configuration (αR) or (αS) of the chiral C-atom of the ligand, together with the four arrangements of the ligand itself in the complex described above for dota complexes. Thus, in the solutions of the the $[\text{Ln}(\text{dotasa})]$ complexes, there can be up to eight stereoisomers of the type $W-X$ ($W = (R)$ or (S) ; $X = M$ ($\Delta(\lambda\lambda\lambda\lambda)$ or $\Lambda(\delta\delta\delta\delta)$) or m ($\Lambda(\lambda\lambda\lambda\lambda)$ or $\Delta(\delta\delta\delta\delta)$), consisting of four enantiomer pairs: (R)- M , (R)- m , (S)- M and (S)- m . Thus, up to four sets of $^1\text{H-NMR}$ signals are to be expected from these enantiomer pairs. The lack of C_4 symmetry removes the signal degeneracy found in the NMR spectra of $[\text{Ln}(\text{dota})(\text{OH}_2)]^-$ complexes and leads to a large number of resonances (25) for each isomer in the $^1\text{H-NMR}$ spectra.

The spectral properties of the paramagnetic Ce^{3+} , Pr^{3+} , Nd^{3+} , Sm^{3+} , Eu^{3+} , and Yb^{3+} chelates of dotasa, as well as of the diamagnetic La^{3+} , Y^{3+} and Lu^{3+} , were investigated by 1D $^1\text{H-NMR}$ and 2D $^1\text{H}, ^1\text{H-COSY}$ experiments. The chelate of the Y^{3+} ion was

included in the present study, as its properties are quite similar to those of the later lanthanides Er^{3+} and Ho^{3+} [29].

The $^1\text{H-NMR}$ spectra of the paramagnetic chelates studied at 25° include a large number of partially overlapping resonances covering paramagnetic shift ranges in accordance with those observed for the corresponding dota chelates [25][27]. The spectra of the Eu^{3+} and Yb^{3+} complexes are the best resolved, where about fifty different resonances could be counted, as expected from the presence of two different isomers of the dotasa chelates. For the earlier lanthanide chelates, about half of the resonances observed have much lower intensities than the others.

Previous $^1\text{H-NMR}$ studies with the symmetrical $[\text{Ln}(\text{dota})(\text{OH}_2)]^-$ chelates, and with a variety of lanthanide derivatives of dota [7], have demonstrated that the two diastereoisomers m and M are present in solution, with a relative proportion that is a function of the lanthanide ion, temperature, solvent, and also the steric crowding of the chelate [7][28]. They are characterized by different dipolar shifts, with complexes of the M form often possessing the larger paramagnetic shifts, for a given ligand resonance.

The full assignment of the complex $^1\text{H-NMR}$ spectra of the paramagnetic lanthanide chelates of dotasa and use of the paramagnetic shifts of the complexes, in particular of Yb^{3+} , in a structural analysis by means of the experimental dipolar shifts, is beyond the scope of the present study. The COSY data obtained were quite complex and not all the assignments could be made. However, a direct information that could be easily obtained from these spectra is the M/m isomer ratio. A particularly useful resonance to observe for this purpose is the most-shifted axial ring proton, ax_1 , which is well-separated from the others [7][8][25–28]. For example, this resonance is observed at *ca.* +30–50 ppm and at *ca.* +150–160 ppm for square antiprismatic (M) Eu^{3+} and Yb^{3+} complexes of dota derivatives at room temperature, while, for the corresponding twisted antiprismatic (m) isomers, the same axial ring proton, ax_1 , has resonances at lower frequencies, at *ca.* +10–30 ppm and *ca.* +90–100 ppm for Eu^{3+} and Yb^{3+} complexes, respectively [7][30–32]. In our study, the ax_1 protons gave two sets of four resonances, well-separated from all the others, in all cases, except for the m isomer of Sm^{3+} , corresponding to the asymmetric M and m isomers, with paramagnetic shifts within the expected ranges (*Fig. 2* and *Table 2*). Integration of those resonances gave the isomer ratios M/m also shown in *Table 2*. Isomer m is dominant for the early lanthanide complexes Ce^{3+} – Nd^{3+} , while for Eu^{3+} up to Yb^{3+} , the M/m ratio stays close to one. A comparison of the observed dependence of the M/m isomer ratio on the ionic radius of the lanthanide ion for the dotasa and dota series of complexes (see below, *Fig. 4*) [28] shows that the α -(carboxymethyl) substituent at one of the acetate arms of dota significantly stabilizes the m isomer relative to M after Nd^{3+} , in particular for the smaller lanthanide ions. An approximate value of the isomer ratio M/m *ca.* 6:1 can be calculated for $[\text{Gd}(\text{dota})(\text{OH}_2)]^-$ by interpolation of the ratios for the Eu^{3+} and Tb^{3+} chelates, while, for $[\text{Gd}(\text{dotasa})(\text{OH}_2)]^{2-}$, a ratio M/m of *ca.* 1:1 can be obtained from those of the Eu^{3+} and Yb^{3+} chelates. It is well-known that the m isomers of lanthanide macrocyclic dota-type chelates have about fifty times faster H_2O exchange rates (k_{ex}) than their M isomers [33–36]. Thus, the much larger abundance of the m isomer for $[\text{Gd}(\text{dotasa})(\text{OH}_2)]^{2-}$ could contribute to explain the 50% increase of H_2O -exchange rate (k_{ex}^{298}) observed for $[\text{Gd}(\text{dotasa})(\text{OH}_2)]^{2-}$ relative to $[\text{Gd}(\text{dota})(\text{OH}_2)]^-$ [9], which

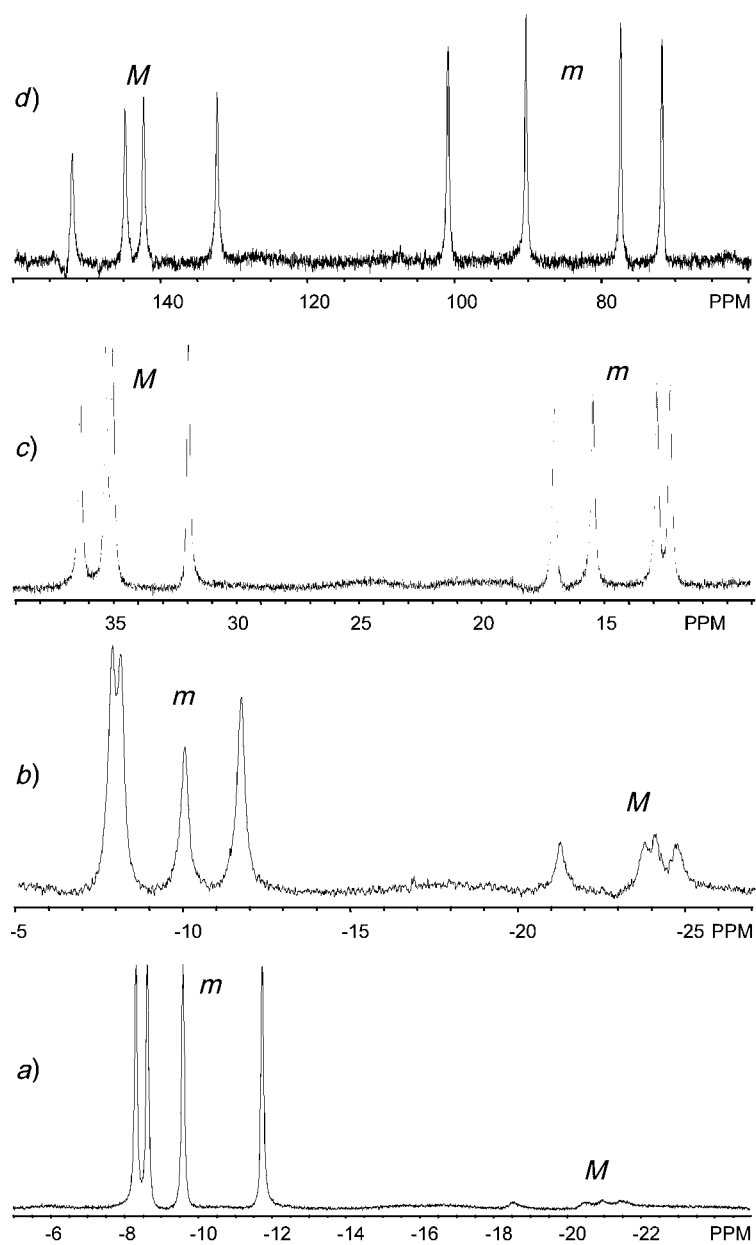


Fig. 2. $^1\text{H-NMR}$ Resonances (D_2O , pH 8.0, 298 K) of the ax_1 protons of the M and m isomers of paramagnetic $[\text{Ln}(\text{dotasa})(\text{OH}_2)]^{2-}$: a) $\text{Ln} = \text{Ce}$, b) $\text{Ln} = \text{Nd}$, c) $\text{Ln} = \text{Eu}$, and d) $\text{Ln} = \text{Yb}$

Table 2. $^1\text{H-NMR}$ Shifts δ [ppm] of the ax_1 Protons of the Paramagnetic $[\text{Ln}(\text{dotasa})(\text{OH}_2)]^{2-}$ Chelates in the M and m Isomeric Forms. Ln = Ce, Pr, Nd, Sm, Eu, and Yb.

	m isomer	M isomer	M/m
Ce	– 8.31, – 8.62, – 9.58, – 11.73	– 18.52, – 20.48, – 20.94, – 21.43	1 : 11.5
Pr	– 23.53, – 23.99, – 27.65, – 30.39	– 40.35, – 46.05, – 46.17, – 46.30	1 : 6.7
Nd	– 7.80, – 8.05, – 9.97, – 11.67	– 21.18, – 23.65, – 23.99, – 24.63	1 : 3.3
Sm	not assigned	– 2.47, – 2.96, – 2.96, – 3.60	–
Eu	17.93, 16.36, 13.76, 13.22	37.28, 36.23, 35.94, 32.85	1 : 0.9
Yb	101.01, 90.44, 77.56, 71.92	152.22, 145.05, 142.52, 132.49	1 : 1.2

was solely attributed before to the extra negative charge in the first complex, resulting in higher proton relaxivity.

The possible presence of the (αR) and (αS) configurations of the substituted pendant arm in the m and M isomers of the dotasa complexes was not reflected in any further splitting of the ax_1 and the other proton resonances of the ligand in the complex, including those from the (carboxymethyl)-substituted acetate arm, as seen in the COSY plot. This has been observed for Ln^{3+} complexes of dota-pnp, dota-like ligand with the $C(\alpha)$ atom of one pendant arm substituted by a p -nitrophenyl group [32], leading to the conclusion that only two of the four possible isomeric species (enantiomer pairs) were present, where the bulky aromatic group was pointing outward from the coordination cage. However, in the case of dotasa, the much less bulky carboxymethyl substituent might adopt also the other configuration, and the presence of the four isomeric species might be masked in the paramagnetic spectra by the very similar geometric factors of the protons in the (αR) and (αS) forms, which determine the large Ln^{3+} induced pseudo-contact shifts. This possibility led us to analyze the spectra of the diamagnetic dotasa complexes.

The proton $^1\text{H-NMR}$ spectra of the diamagnetic La^{3+} , Y^{3+} , and Lu^{3+} complexes of dotasa (data not shown), although very crowded in the 5.0–2.6 ppm region, reveal the presence of the stereoisomeric (αR) and (αS) forms of the substituted pendant arm. The isomer ratio obtained for the Ce^{3+} complex indicates that the spectrum of $[\text{La}(\text{dotasa})(\text{OH}_2)]^{2-}$ should be dominated by the resonances of the m isomer. Its COSY plot (Fig. 3, a) shows many cross-peaks, but those involving the $\text{CH}(c)$ and $\text{CH}_2(d)$ protons (see, Fig. 1) of the (carboxymethyl)-substituted acetate pendant arm are easily assigned. Two strong ABX spin systems (CH at 4.50 and CH_2 at 2.84 and 2.68 ppm; CH at 4.12 and CH_2 at 3.48 and 3.40 ppm) are assigned to the major (R)- m and (S)- m isomers. The three sets of CH_2 protons of the nonsubstituted acetate pendant arms originate a cluster of nearly overlapping cross-peaks corresponding to six different AX systems (at 4.2–3.8 and 3.3–3.1 ppm), reflecting the (αR) and (αS) configurations at the substituted arm of the m isomer. Other much less intense cross-peaks of the substituted (ABX) (e.g., at 4.12, 2.90, and 2.54 ppm) and unsubstituted (AX) acetate arms (e.g., at 3.80–3.52 and 3.65–3.20 ppm) are also present, corresponding to the minor (R)- M and (S)- M isomers. The ring protons give a large number of partially overlapping cross-peaks that were not assigned. The Y^{3+} and Lu^{3+} dotasa complexes originate much more-complex 1D $^1\text{H-NMR}$ and COSY plots (Fig. 3, b). The presence of a much larger number of cross-peaks in the COSY plots

reflects the presence of four (*(R)*-*m*, (*(S)*-*m*, (*(R)*-*M*, and (*(S)*-*M*) isomers with comparable populations, as expected from the isomer ratios obtained for the paramagnetic complexes. This is clearly illustrated by the presence of cross-peaks from four *ABX* systems corresponding to the CHCH₂ protons of the α -substituted arm, with CH resonances at 4.42, 4.21, 4.02, and 3.85 ppm correlated with signals at 2.65–2.75 ppm, and the large number of heavily overlapping cross-peaks of the CH₂ protons of the other three acetate arms.

Exchange between the *m* and *M* isomers of the dotasa chelates is demonstrated by the broadening and collapse of the resonances of both isomers observed at 70°, both for the diamagnetic and paramagnetic complexes, but the kinetics of the process was not studied further [26].

It is worth comparing the present conclusions on the number and type of isomers for the [Ln(dotasa)(OH₂)]²⁻ complexes with previous NMR studies of lanthanide chelates of symmetrical and non-symmetrical derivatives of dota, modified at the acetate C(α) and/or the tetraaza ring [7]. A very similar case to the present study with dotasa is the introduction of only one chiral center in dota by derivatizing one acetate C(α) with a *p*-nitrophenyl group, resulting in a nonsymmetrical dota derivative, *i.e.*, (*RS*)-dota-pnp [32]. The ¹H-NMR spectra of its Ho³⁺ and Yb³⁺ complexes show the presence of only two of the four possible isomers, with *M/m* ratios (88:12 and 3:1, resp.) indicating that the population of the *m* isomer is only slightly increased relative to the corresponding [Ln(dota)(OH₂)]⁻ chelates (Fig. 4), indicating that a bulky substituent at an acetate arm (such as in dota-pnp) has a much lower stabilizing effect on the *m* isomer than a flexible, less bulky one (such as in dotasa).

In the case of symmetrical C(α)-substitution, the introduction of four identical chiral centers of (*R*) or (*S*) configuration in the acetate arms of dota may produce twelve stereoisomers (six enantiomer pairs), resulting from the combinations of the C(α) configurations (*(R,R,R,R)*, *(R,R,R,S)*, *(R,R,S,S)*, *(R,S,R,S)*, *(R,S,S,S)*, and *(S,S,S,S)* with a 1:4:4:2:4:1 statistical relative intensity) and the helicity (Δ/Λ) of the pendant arms. However, the number of isomers actually observed in the tetrasubstituted dota derivatives is sometimes much lower. In the case of the ligand (*R,R,R,R*)-dotma, where the C(α) atom of each acetate arm is substituted with a Me group generating (*aR*) configuration, the ¹H-NMR spectrum of [Yb(dotma)(OH₂)]⁻ shows only two isomers, *m* and *M*, resulting from the helicity (Δ/Λ) of the pendant arms, with (*R,R,R,R*) configuration [37]. The presence of the four Me–C(α) again increases the rigidity of the chelate and makes the *m* isomer dominant relative to *M* in [Yb{(*R,R,R,R*)-(dotma)}(OH₂)]⁻ (*m/M* \approx 15:1, compare with the other chelates in Fig. 4) [37]. The (*R,R,R,R*), (*R,R,R,S*), (*R,R,S,S*) and (*R,S,R,S*) stereoisomers of the [Eu(tce-dota)(OH₂)]³⁻ complex, where tce-dota is the symmetrically substituted $\alpha,\alpha',\alpha'',\alpha'''$ -tetrakis(carboxyethyl) derivative of dota, were individually analyzed by ¹H-NMR in solution, to study their isomeric composition [30][31]. The *M/m* ratios obtained were 1:0 (*R,R,S,S*) > 4:1 (*R,S,R,S*) > 2:1 (*R,R,R,S*) > 1:4 (*R,R,R,R*), showing that in the first two cases, the absolute configuration of the chiral C(α) centres does not significantly affect the stereoisomer *M/m* ratio found for [Eu(dota)(OH₂)]⁻, but for the less symmetric (*(R,R,R,S)*) and especially (*(R,R,R,R)*) isomers, the C(α) centres determine the left-handed helicity of the complexes, favoring the *m* isomer [30][31]. For the (*R,R,R,R*) isomer, the *m* form predominates along the

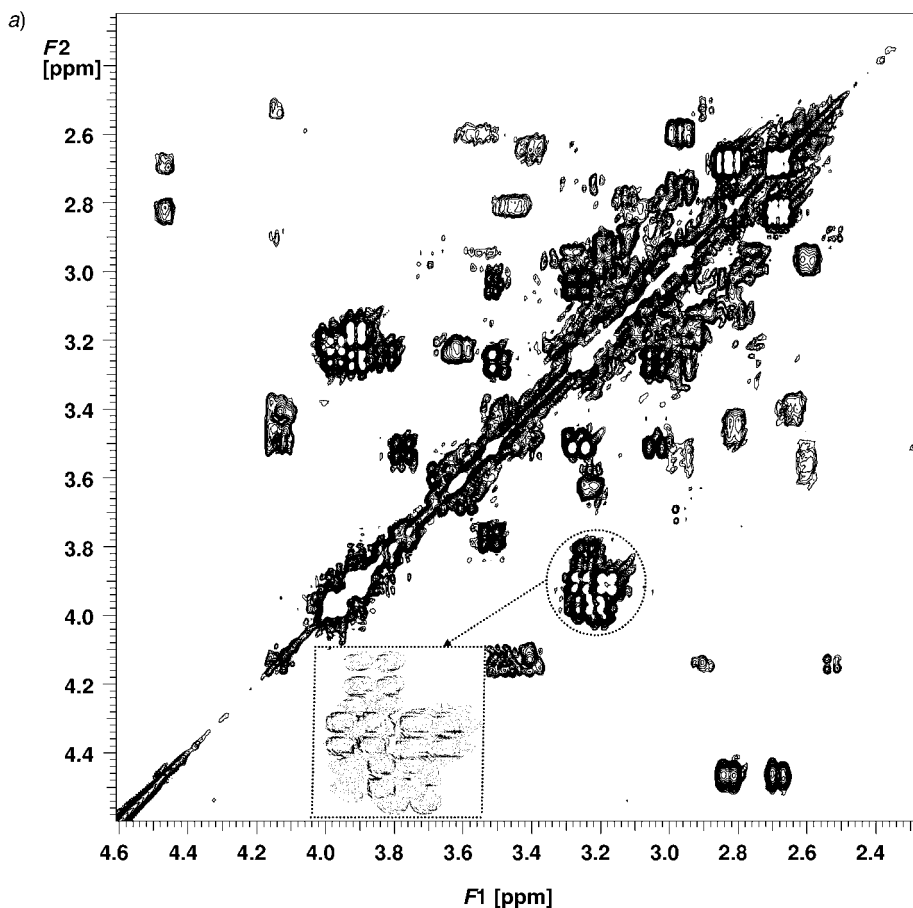


Fig. 3. COSY Plots (D_2O , pH 8.0, 298 K) of $[\text{Ln}(\text{dotasa})(\text{OH}_2)]^{2-}$: a) $\text{Ln} = \text{La}$, b) $\text{Ln} = \text{Lu}$

lanthanide series, but changes differently from the $[\text{Ln}(\text{dota})(\text{OH}_2)]^-$ or $[\text{Ln}(\text{dotasa})(\text{OH}_2)]^{2-}$ series, with a minimum at Tb^{3+} (Fig. 4).

If dota derivatization at the acetate arms affects the isomer ratio in ways that depend on the relative configuration of the substituents, its derivatization at the tetraaza ring has a dominant effect on the isomers formed, as shown also by $^1\text{H-NMR}$ [38]. The Yb^{3+} complex of the four-fold symmetric (R,R,R,R) - m_4 dota ligand, with four Me substituents at the tetraaza ring, shows three isomers M , m , and m' in the ratio 1:0.095:0.013. The orientation of the Me groups has a large influence on the stability of the square antiprismatic (M) and twisted antiprismatic (m , m') structures, as their 'equatorial up' orientation (present in the M and m isomers) is much more stable than the 'equatorial down' orientation (m' isomer) [38]. Here, the dominance of the M isomer in $[\text{Yb}(\text{dota})(\text{OH}_2)]^-$ is maintained in $[\text{Yb}\{(R,R,R,R)\text{-}(m_4\text{dota})\}(\text{OH}_2)]^-$. The Yb^{3+} complex of the nonsymmetric racemic (R/S) - m dota ligand, monomethylated at the tetraaza ring, has four isomers, with relative intensities M (M -eq up) $>$ m' (m -eq

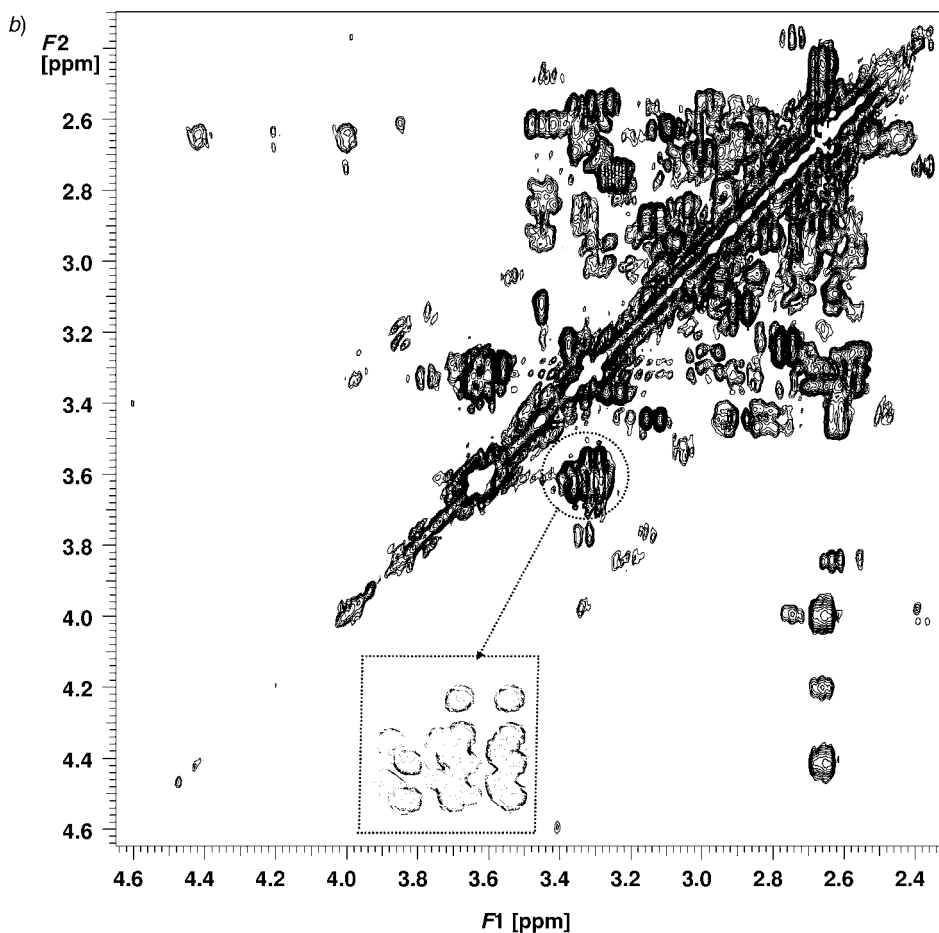


Fig. 3 (cont.)

down) $\gg M'$ (M -eq down) $> m$ (m -eq up) [38]. Here the orientation of the ring Me group is more important than the helicity of the acetate arms in determining the stability of the isomers. Finally, the Yb^{3+} complex of the symmetric $m_4\text{dotma}$ ligand, with four Me substituents each at the tetraaza ring and at the acetate arms in the (S,S,S,S) and (R,R,R,R) configurations, respectively, features a ^1H -NMR spectrum with only one isomer, M (M -eq up) [38]. Again, the most stable orientation of the ring Me groups dominates, inverting the helicity of the most stable isomer (m) in $[\text{Yb}\{(R,R,R,R)\text{-}(m_4\text{dota})\}(\text{OH}_2)]^-$.

3. Conclusions. – The present studies with the ligand H_5dotasa , where one $\text{C}(\alpha)$ of an acetate arm is substituted by a carboxymethyl group ($\alpha R/\alpha S$ racemic mixture), further illustrate the multiple effects that derivatization of the H_4dota ligand has on the properties of the corresponding Gd^{3+} chelate, with consequences on its potential

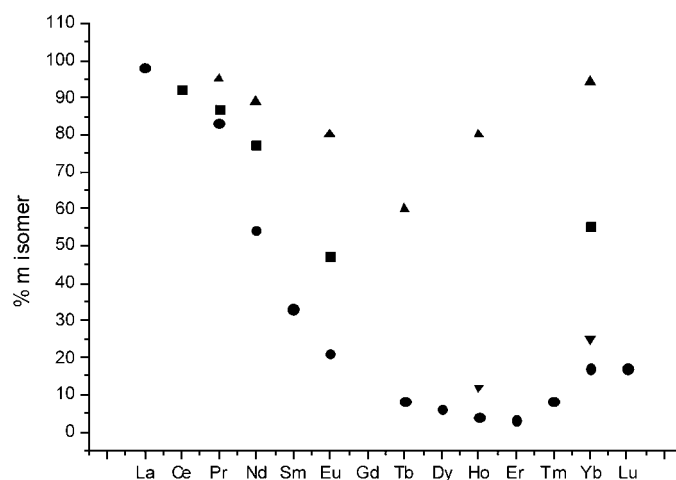


Fig. 4. Molar fractions of the isomer *m* for [Ln(tetraazamacrocycles)] in aqueous solution (pH 7, 298 K), as a function of the complex metal ion obtained from ¹H-NMR: [Ln(dotasa)]²⁻ (■; this work), [Ln(dota)(OH₂)]⁻ (●; [11][25]), [Ln(R,R,R,R)-(tce-dota)(OH₂)]⁵⁻ (▲; [31]), [Ln(dota-pnp)(OH₂)]⁻ (▼; [32])

application as an MRI contrast agent. While the protonation constants of H₅dotasa are not much changed relative to H₄dota except for an extra p*K* value due to protonation of the extra carboxylate group in the *α*-substituted arm, the stability constant of its Gd³⁺ chelate is significantly increased relative to [Gd(dota)(OH₂)]⁻. The number of isomers in solution of the Ln³⁺ chelates of dotasa also doubles, combining the *M* and *m* structures of the framework of the complexes with the (*αR*) and (*αS*) configurations of the substituted pendant arm. More importantly, the *m*-isomer population of the Gd³⁺ complex with dotasa is 3–4 times increased relative to [Gd(dota)(OH₂)]⁻. This is in contrast with the C(*α*) effect of the sterically more bulky *p*-nitrophenyl group, like in the [Gd(dota-pnp)]⁻ chelate [32], where the % *m* increase is much smaller. The effect of the flexible carboxymethyl group in [Gd(dotasa)(OH₂)]⁻ on the % *m* increase is almost as high as that resulting from (*R,R,R,R*)-tetrasubstitution of dota [31], and can thus be considered a good strategy of connecting a [Gd^{III}-(tetrazamacrocycle)] to a carrier while increasing its H₂O-exchange rate, and thus its relaxivity.

The work was supported by the *Foundation of Science and Technology (F. C. T.)*, Portugal (project POCTI/QUI/47005/2002), *FEDER*, the *Hungarian Science Foundation (OTKA T038364)*, and the *Swiss National Science Foundation*. It was performed within the framework of the *EU COST Action D18* 'Lanthanide chemistry for diagnosis and therapy'.

Experimental Part

General. The ligand H₃dotasa was prepared, isolated, and purified as a racemic mixture of the (*αR*) and (*αS*) enantiomers as described elsewhere [9]. It was used in the form C₁₈H₃₀N₄O₁₀ · 2.30 HCl · 1.73 H₂O · NaBr, as obtained by elemental analysis [9]. The lanthanide chlorides, other salts and deuterated solvents were obtained from *Sigma*. The Ln³⁺ and Y³⁺ complexes (Ln = La, Lu, Pr, Nd, Sm, Eu, and Yb) for NMR studies were prepared by adding a D₂O soln. containing 40 mmol (1 equiv.) of the ligand to the same volume of an equimolar soln. of LnCl₃ in D₂O. The pH of the solns. was slowly adjusted to 7–8 with aq. KOD soln.

Potentiometric Titrations. Ligand solns. were titrated in a thermostated cell under a stream of N₂ with a 0.5M standard soln. of Me₄NOH (standardized with potassium hydrogenphthalate) at an ionic strength adjusted to

0.50M with Me_4NNO_3 in a *Metrohm 665-Dosimat* with a 1-ml piston burette. Excess nitric acid was added to the ligand solns. (25 ml, 1.5 mM) to determine the lower protonation constants. All the solns. were prepared with deionized H_2O (*Millipore*) which was previously boiled to remove the CO_2 . pH Measurements were carried out with a *Metrohm 654* digital pH meter equipped with a *Metrohm 0.0204.100* glass electrode combined with a calomel (3M KCl) reference electrode. The glass electrode was calibrated with pH 4.0 and 7.0 buffers at 25°. The pH meter/electrode system was calibrated by titration of a 3.2 mM *Tris* soln. with 0.5M Me_4NOH soln. at an ionic strength adjusted to 0.5M with Me_4NNO_3 . The data were handled and calculated with the program TITFIT [39].

Another set of potentiometric measurements was performed by using a ionic strength of 0.10M in Me_4N . For the potentiometric determination of the stability constant of $[\text{Gd}(\text{dotasa})]^{2+}$, 20 samples of 4.00-ml volume were prepared. The concentrations of the Gd^{3+} ion and of the ligand were the same: 0.005M. The pH values were between 1.8 and 2.4 at equilibrium. These 'out of cell' samples were kept at 60° for 2 days, then at 40° for 4 days, and finally at 25° for 2 weeks. The fitting parameter related to 20 data pairs is 0.007 ml. The standard deviation is a little bit higher than usual, but even the stability constant is high. The pH measurements were carried out with a *PHM85 Radiometer* pH meter and with a combined electrode *6.0234.100 (Metrohm)*. The effect of the liquid-junction potential of the electrode was taken into consideration. For obtaining H^+ -ion concentration from the measured pH values, the method suggested by *Irving et al.* [40] was used.

The value $\text{p}K_a = 13.89$, which was determined in our cell, was also used for calculations. For the computation, the software PSEQUAD [41] was used.

A sample of pH 2.07 containing 0.0005M Ce^{III} and dotasa was also measured together with the studied systems. The changes in this soln. were followed spectrophotometrically with a *Cary-1E* spectrophotometer.

NMR Experiments. $^1\text{H-NMR}$ Spectra: *Varian Unity-500* spectrometer; probe temp. accurate to $\pm 1^\circ$; D_2O solns. (vs. sodium 3-(trimethylsilyl)propanesulfonate (TSP)). Solns. of H_3dotasa (0.08M) for NMR pH titrations were prepared in D_2O and the pD was adjusted with DCl or KOD. The final pH was determined with a *Hanna 8417* pH meter fitted with a combined *Hanna HI1310* electrode and calibrated at $20 \pm 1^\circ$ with two standard buffers at pH 4.0 and 7.0 and corrected for the deuterium isotope effect by using $\text{pH} = \text{pD} - 0.4$ [42]. 1D $^1\text{H-NMR}$ spectra and 2D COSY plots were recorded as a function of added base.

Solns. of the diamagnetic (La^{3+} , Lu^{3+} , and Y^{3+}) and paramagnetic (Ce^{3+} , Pr^{3+} , Nd^{3+} , Sm^{3+} , Eu^{3+} , and Yb^{3+}) metal-ion complexes of dotasa for NMR measurements contained 40 mM of ligand and 1 equiv. of the trivalent metal chloride in D_2O adjusted to pH 7–8 with DCl or KOD. 1D $^1\text{H-NMR}$ and 2D COSY plots of the complexes were obtained at 25° and 70° under presaturation (transmitter and decoupler, resp.) to suppress the residual water solvent signal.

REFERENCES

- [1] P. Caravan, J. J. Ellison, T. J. McMurry, R. B. Lauffer, *Chem. Rev.* **1999**, *99*, 2293.
- [2] S. Aime, M. Botta, M. Fasano, E. Terreno, *Chem. Soc. Rev.* **1998**, *27*, 19.
- [3] D. Parker, J. A. G. Williams, *J. Chem. Soc., Dalton Trans.* **1996**, 3613.
- [4] J. B. Stimmel, F. C. Kull, *Nuclear Med. Biol.* **1998**, *25*, 117.
- [5] T. J. Norman, F. C. Smith, D. Parker, A. Harrison, L. Royle, C. A. Walker, *Supramol. Chem.* **1995**, *4*, 305.
- [6] C. F. G. C. Geraldès, *Top. Curr. Chem.* **2002**, *221*, 26.
- [7] J. A. Peters, E. Zitha-Bovens, D. Corsi, C. F. G. C. Geraldès, 'Structure and Dynamics of Gadolinium-Based Contrast Agents', in 'The Chemistry of Contrast Agents in Medical Magnetic Resonance Imaging', Eds. É. Tóth and A. E. Merbach, Wiley, Chichester, 2001, p. 315.
- [8] J. F. Desreux, *Inorg. Chem.* **1980**, *19*, 1319.
- [9] J. P. André, É. Tóth, H. R. Maecke, A. E. Merbach, *J. Biol. Inorg. Chem.* **1999**, *4*, 341.
- [10] J. P. André, É. Toth, H. Fischer, A. Seelig, H. R. Maecke, A. E. Merbach, *Chem. Eur. J.* **1999**, *5*, 2977.
- [11] S. Aime, M. Botta, M. Fasano, M. P. M. Marques, C. F. G. C. Geraldès, D. Pubanz, A. E. Merbach, *Inorg. Chem.* **1997**, *36*, 2059.
- [12] S. Aime, M. Botta, E. Garino, S. G. Crich, G. Giovenzana, R. Pagliarin, G. Palmisano, M. Sisti, *Chem.–Eur. J.* **2000**, *6*, 2609.
- [13] R. Delgado, J. J. R. Frausto da Silva, *Talanta* **1982**, *29*, 815.
- [14] K. Kumar, C. A. Chang, L. C. Francesconi, D. D. Dischiro, M. F. Malley, J. Z. Gougoulas, M. F. Tweedle, *Inorg. Chem.* **1994**, *33*, 3567.
- [15] A. Bianchi, L. Calabi, C. Giorgi, P. Losi, P. Mariani, P. Paoli, P. Rossi, B. Valtancoli, M. Virtuani, *J. Chem. Soc., Dalton Trans.* **2000**, 697.

- [16] J. F. Desreux, E. Merciny, M. F. Loncin, *Inorg. Chem.* **1981**, *20*, 987.
- [17] J. L. Sudmeier, C. N. Reilley, *Anal. Chem.* **1964**, *36*, 1698.
- [18] C. F. G. C. Geraldes, A. M. Urbano, M. C. Alpoim, A. D. Sherry, K.-T. Kuan, R. Rajagopalan, F. Maton, R. N. Muller, *Magn. Reson. Imaging* **1995**, *13*, 401.
- [19] C. F. G. C. Geraldes, M. C. Alpoim, M. P. M. Marques, A. D. Sherry, M. Singh, *Inorg. Chem.* **1985**, *24*, 3876.
- [20] J. R. Ascenso, R. Delgado, J. J. R. Frausto da Silva, *J. Chem. Soc., Perkin Trans. 2* **1985**, 781.
- [21] C. F. G. C. Geraldes, A. D. Sherry, M. P. M. Marques, M. C. Alpoim, S. Cortes *J. Chem. Soc., Perkin Trans 2* **1991**, 137.
- [22] C. F. G. C. Geraldes, A. D. Sherry, W. P. Cacheris, *Inorg. Chem.* **1989**, *28*, 3336.
- [23] R. R. Ranganatham, R. K. Pillai, N. Raju, H. Fan, H. Nguyen, M. F. Tweedle, J. F. Desreux, V. Jacques, *Inorg. Chem.* **2002**, *41*, 6846.
- [24] É. Tóth, E. Brücher, I. Lázár, *Inorg. Chem.* **1994**, *33*, 4070.
- [25] S. Aime, B. Botta, G. Ermondi, *Inorg. Chem.* **1992**, *31*, 4291.
- [26] V. Jacques, J. F. Desreux, *Inorg. Chem.* **1994**, *33*, 4048.
- [27] M. P. M. Marques, C. F. G. C. Geraldes, A. D. Sherry, A. E. Merbach, A. E. Powell, D. Pubanz, S. Aime, B. Botta, *J. Alloys Compd.* **1995**, 225, 303.
- [28] S. Aime, B. Botta, M. Fasano, M. P. M. Marques, C. F. G. C. Geraldes, D. Pubanz, A. E. Merbach, *Inorg. Chem.* **1997**, *36*, 2059.
- [29] F. A. Cotton, G. Wilkinson, C. A. Murillo, M. Bochmann, 'Advanced Inorganic Chemistry', Wiley, New York, 1999.
- [30] J. A. K. Howard, A. M. Kenright, J. M. Moloney, D. Parker, M. Woods, M. Port, M. Navet, O. Rousseau, *J. Chem. Soc., Chem. Commun.* **1998**, 1381.
- [31] M. Woods, S. Aime, M. Botta, J. A. K. Howard, J. M. Moloney, M. Navet, D. Parker, M. Port, O. Rousseau, *J. Am. Chem. Soc.* **2000**, *122*, 9781.
- [32] S. Aime, M. Botta, G. Ermondi, E. Terreno, P. L. Anelli, F. Fedeli, F. Uggeri, *Inorg. Chem.* **1996**, *35*, 2726.
- [33] S. Aime, A. Barge, M. Botta, A. S. de Sousa, D. Parker, *Angew. Chem., Int. Ed.* **1998**, *37*, 2673.
- [34] S. Aime, A. Barge, J. I. Bruce, M. Botta, J. A. K. Howard, J. M. Moloney, D. Parker, A. S. de Sousa, M. Woods, *J. Am. Chem. Soc.* **1999**, *121*, 5762.
- [35] A. F. Dunand, S. Aime, A. E. Merbach, *J. Am. Chem. Soc.* **2000**, *122*, 1506.
- [36] É. Tóth, L. Helm, A. E. Merbach, 'Structure and Dynamics of Gadolinium-Based Contrast Agents', in 'The Chemistry of Contrast Agents in Medical Magnetic Resonance Imaging', Eds. É. Tóth and A. E. Merbach, Wiley, Chichester, 2001, p. 45.
- [37] H. G. Brittain, J. F. Desreux, *Inorg. Chem.* **1984**, *23*, 4459.
- [38] R. R. Ranganatham, N. Raju, H. Fan, X. Zhang, M. F. Tweedle, J. F. Desreux, V. Jacques, *Inorg. Chem.* **2002**, *41*, 6856.
- [39] A. D. Zuberbühler, T. A. Kaden, *Talanta* **1982**, *29*, 201.
- [40] H. M. Irving, M. G. Miles, L. Pettit, *Anal. Chim. Acta* **1967**, *38*, 475.
- [41] L. Zékány, I. Nagypál, in 'Computational Methods for Determination of Formation Constants', Ed. D. J. Leggett, Plenum, New York, 1985, p. 291.
- [42] P. K. Glasoe, F. A. Long, *J. Phys. Chem.* **1960**, *64*, 188.

Received November 4, 2004